NUMERICAL STUDY ON ABRASIVE WEAR OF RECIPROCATING SEALS UNDER MIXED LUBRICATION CONDITIONS

Jiehao Wang[1], Jing Li[1]*, Yaobao Yin[1]

[1] *School of Mechanical Engineering, Tongji University, Caoan Road 4800, 201804 Shanghai*

* Corresponding author: Tel.: +86 18964895619; E-mail address: cynthia_li@tongji.edu.cn

ABSTRACT

The reciprocating seals of the actuator are under mixed lubrication conditions, where rough peak contact and oil film lubrication coexist. The seal wear during operation has a severe impact on its sealing performance. The actual wear phenomena usually include many forms, such as abrasive wear, adhesive wear, etc. The classical Archard model based on adhesive wear theory is commonly used for seal wear analysis, while research on abrasive wear is still rare. This study establishes a three-body micro-contact model of the piston rod, abrasive and wear ring based on fractal theory and finite element simulation to analyze the contact characteristics of abrasives in the sealing separation. The influence of fractal surface parameters, abrasive size, shape, and material hardness on abrasive motion, contact, and friction stress are investigated. Next, the percolation channel model of the sealing surface is established to investigate the mechanism of topography characteristics on the leakage after wear. The calculation model and method for reciprocating seal leakage can be obtained based on percolation theory. This model and theoretical analysis aim to clarify the wear failure life assessment, full life cycle management, and anti-degradation design of reciprocating seals.

Keywords: Reciprocating seal, Mixed lubrication, Abrasive wear, Surface topography, Percolation theory

1. INTRODUCTION

The reciprocating seal is a prevalent sealing mechanism in hydraulic systems, extensively applied across diverse fields such as aerospace, engineering machinery, and the chemical and pharmaceutical industries. This seal type is highly valued for its low leakage rate, superior reliability, and broad applicability. The core components of a reciprocating seal typically include an O-ring, a wear ring, and various auxiliary components. During the seal's operation, relative motion is produced between the wear ring and the piston rod surface, leading to friction [1,2]. The reciprocating seal's performance is contingent upon maintaining its sealing capability during the reciprocating motion while minimizing friction to limit wear.

Abrasive wear is a phenomenon wherein external hard particles, protruding objects, or surface rough peaks cause surface material to dislodge during friction [3]. There are three main types of abrasive wear: (1) Two-body abrasive wear occurs when abrasive particles move relative to a solid surface, producing scratches or furrows on the surface according to the direction of abrasive movement; (2) Low-stress abrasive wear is observed in a pair of friction pairs when the rough peak of the hard surface rides the abrasive particle on the softer surface; (3)Three-body abrasive wear occurs when external wear particles or metal particles move between two friction surfaces, generating extremely high contact stress and causing the surface material to spall [4].

Reciprocating seals, typically employing contact sealing, are particularly prone to abrasive wear due

to the working conditions. The seal gap allows the percolation of lubricating oil, placing the sealing surface in a mixed lubrication state, where the compressed oil and rough peaks bear the normal load, as shown in **Figure 1**. Long-term operation of the hydraulic system can produce tiny metal particles that flow into the sealing system with the oil, leading to a medium rich in impurities. The primary failure mode is severe sealing surface wear, leading to percolation channel formation and significant leakage. This can easily result in substantial leaks and rapid seal failure, drastically reducing the service life of the reciprocating seal [5]. The amount of wear produced by abrasive wear depends on the abrasive particles' hardness, strength, shape, sharpness, and size. Wear of the seal alters the topography of the sealing surface, producing separation in areas where continuous contact clusters form on the original sealing surface. These gaps can create percolation channels through the sealing surface, resulting in seal failure and leakage [6,7]. Thus, investigating the surface topography, deformation, friction, and wear mechanism of the reciprocating seal end face under abrasive wear conditions is of substantial importance.

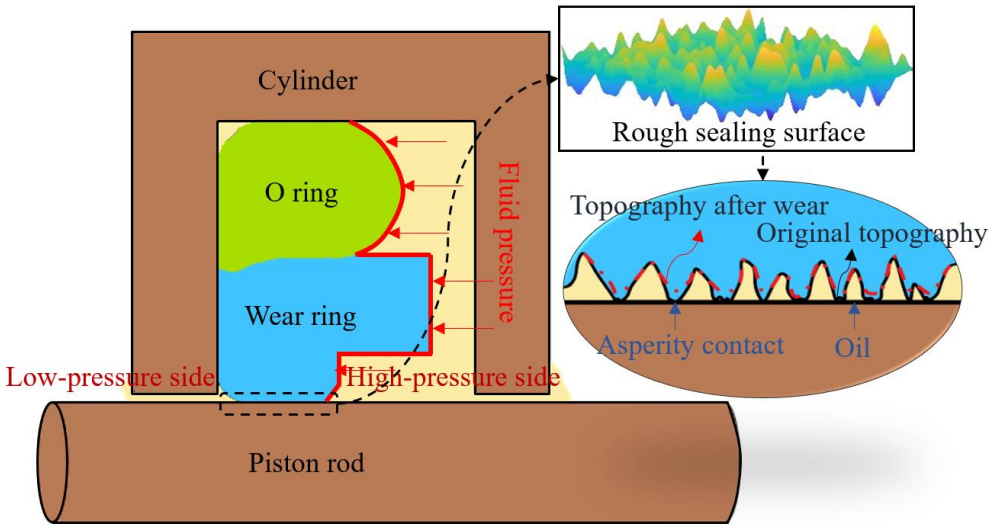

Figure 1: Working condition of the reciprocating seal

The sealing surface topography evaluates the seal's processing and manufacturing and helps explore the nature of lubrication, contact, and wear mechanisms. The fractal theory provides a practical tool for modelling the contour curve of a rough surface [8]. The advantage is its independence from the measurement scale, and the simulated curve exhibits regularity, making it suitable for mathematical model calculations of friction and wear under mixed lubrication. Under abrasive conditions, the friction pair often transitions from two- to three-body wear [9,10]. It has been observed that abrasive particles become embedded in the polytetrafluoroethylene (PTFE) friction pairs used for sealing, causing wear on the surface of the metal piston rod. Finite element and numerical analysis can effectively analyze the sealing surface's motion mode, stress-strain, and pressure changes during wear.

The influence mechanism of the rough surface profile parameters of the wear ring and topography evolution following wear on sealing performance should be considered. However, the current study calculates the leakage rate by studying the oil film thickness of the sealing surface using the average Reynolds equation [11]. This approach only allows for an estimate of the leakage state and fails to reflect the sealing nature of the continuous contact area on the sealing surface to prevent oil leakage. In this study, we propose combining percolation theory with the topography evolution of the sealing surface, constructing a sealing leakage channel to determine the flow rate at the critical constriction, and calculating the leakage amount. When combined with the friction and wear mechanism, this method enables the construction of a microscale reciprocating sealing leakage analysis method.

2. NUMERICAL MODEL

2.1. Fractal theory

Every machined surface, when magnified sufficiently, reveals a degree of roughness. This is true for the sealing surface as well, and as such, when sealing surfaces make contact, they only do so at specific points. The non-contact areas connect to form a percolation channel, the fundamental source of leakage. On a microscopic scale, the stress and deformation of the contact points and the percolation channel's size and distribution are intimately linked to the surface topography.

Currently, the usage of fractal theory to study topography relies on the Weierstrass-Mandelbrot (W-M) function. This function exhibits randomness, self-similarity, and continuity and is non-differentiable at all points, which aligns perfectly with the traits of machined surface contours [12,13]. The expression for the three-dimensional fractal surface model in the Cartesian coordinate system is:

$$z(x,y)=L\left(\frac{G}{L}\right)^{D-2}\left(\frac{\ln\gamma}{M}\right)^{1/2}\sum_{m=1}^{M}\sum_{n=0}^{n_{\max}}\left(k\gamma^{n}\right)^{D-3} \times\left\{\cos\phi_n-\cos\left[\frac{2\pi\gamma^{n}\left(x^{2}+y^{2}\right)^{1/2}}{L}\times\cos\left(\tan^{-t}\left(\frac{y}{x}\right)-\frac{\pi m}{M}\right)+\phi_n\right]\right\} \tag{1}$$

where the variables x, y, z represent the horizontal coordinates, vertical coordinates, and surface height, respectively; M represents the number of superimposed wave layers in the fractal surface; L is the sample length; γ^n denotes the spatial frequency; n is the frequency base number; ϕ_n is a random number between 0 and 2π for the superposition of waves; D is a fractal dimension, represents the number of fractal cones; G is the scale parameter, indicating the relative height of the surface features. This model provides a comprehensive mathematical representation of the surface topography, allowing for the nuanced characterization of a rough surface's topography characteristics. When M is set to 1 and y to 0, the three-dimensional fractal surface model can be simplified to obtain a two-dimensional contour function of the fractal surface in the X-Z plane, which is

$$z(x)=L\left(\frac{G}{L}\right)^{D-2}\left(\frac{\ln\gamma}{M}\right)^{1/2}\sum_{n=0}^{n_{\max}}\gamma^{(D-3)n}\left[\cos\phi-\cos\left(\frac{2\pi\gamma^{n}x}{L}-\phi\right)\right] \tag{2}$$

Since the roughness of the piston rod is significantly smaller than that of the wear ring, the sealing contact surface of the reciprocating seal can be approximated as the extrusion contact between a fractal surface and a smooth, rigid surface. The following assumptions are adopted to simplify the contact process [14]: (a) the fractal surface is isotropic; (b) the contact at the asperities follows the Hertzian contact hypothesis, and the asperities are spherical; (c) the axial deformation between the asperities is ignored. The curvature radius of a single asperity can be determined as follows:

$$R=\left|\frac{1}{\left|d^{2}z/dx^{2}\right|_{x=}}\right|=\frac{l^{(D-1)}}{4\pi^{2}G^{(D-2)}\left(\ln\gamma\right)^{1/2}} \tag{3}$$

where l represents the base wavelength of the asperity on the reference plane. Once the contact is quantified, contact stress distribution can be determined using classical contact mechanics models.

2.2. Abrasive wear

In this study, only the wear of the wear ring is considered while disregarding the wear of the piston rod. There are three main wear mechanisms: (a) The normal load will force the abrasive pressure on the surface, and the surface will be cut through the furrow action of the abrasive in relative motion.

(b) The abrasive particles move between the two contact surfaces, like cutting tools, causing wear on the softer surface; (c) The abrasive particles move quickly between the two contact surfaces, producing an impact force on the friction surface and resulting in wear. Generally, the rod speed of the actuator is not too large, and the wear forms are mainly the first two. The Archard model quantitatively describes the correlation between the wear volume of material and variables such as load, sliding distance, and hardness [15]. This model has been extensively employed in studies related to seal wear due to its simplicity and accuracy under certain conditions, and its expression is

$$W_a = \frac{K_a F_N s}{H_m} \tag{4}$$

where W_a is the wear volume, K_a is the wear coefficient, F_N is the nominal load, s is the sliding distance, and H_m is the hardness of the softer material. The Archard's model can also be modified to calculate the wear depth at a specific location, that is

$$h_w = k_a p_c s \tag{5}$$

where $k_a = K_a / H_m$ is the non-dimensional wear coefficient, p_c is the asperity pressure. In addition, a finite element analysis (FEA) model for Archard wear can be established by incorporating the APDL command flow into the contact pair of the piston rod and wear ring. The operating conditions for the FEA model are depicted in **Figure 2**. The wear volume on the rough surface of the wear ring can be calculated to obtain the topograph evolution of the wear ring's surface over time.

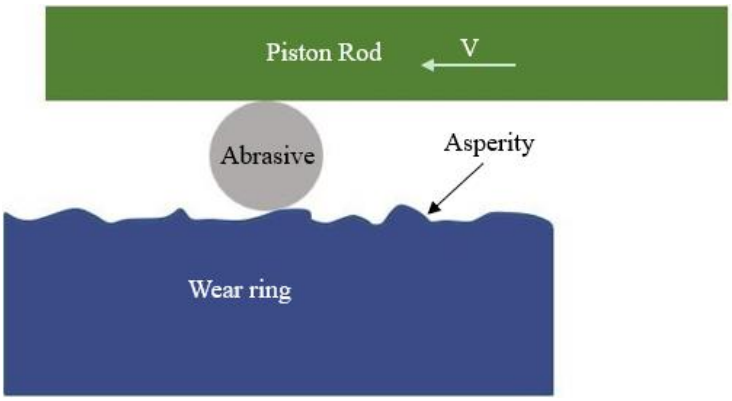

Figure 2: FEA model of abrasive wear

In the context of a contact problem between a smooth, rigid surface and an elastomeric rough surface, the calculation can be performed based on the elastic deformation of the asperities on the surface. The elastic deformation of an asperity can be represented as:

$$\omega = \sigma_a - h \tag{6}$$

where $\sigma_a = z(l/2)$ is the asperity height, h is the separation between the fundamental plane of the rough surface and the rigid plane. According to [16], it is crucial to evaluate whether the asperity deformation is less than the critical deformation associated with elastic deformation. The material properties and contact conditions determine the critical deformation of the asperity, that is

$$\omega_e = \left(\frac{\pi K_h H_m}{2E}\right)^2 R = \left(\frac{K_h \phi}{4}\right)^2 \frac{l^{D-1}}{G^{D-2}\sqrt{\ln \gamma}} \tag{7}$$

where K_h is the hardness coefficient of the material, generally obtained by empirical formula $K_h = 0.454 + 0.41\nu$, ν is the Poisson ratio of the material, H_m and E is the Brinell hardness and elastic modulus, respectively, determined by the material characteristics. The contact pressure generated by the elastic deformation of the asperity is:

$$p_c = \frac{4E}{3\pi}\sqrt{\frac{\omega}{R}} \tag{8}$$

2.3. Percolation theory

The leakage condition in a contact seal occurs when the gaps on the sealing surface interconnect to create a percolation channel across the surface. Since the irregular interaction of asperities on the sealing surface, the separation presents a complex and random shape. The percolation theory describes fluid's random transfer and flow process in random porous media. The formation of a percolation channel is related to the magnification factor of the sealing surface [17]. As the magnification factor ζ increases, more roughness details become evident, and the contact area on the sealing surface correspondingly decreases.

The critical magnification factor ζ_c represents the magnification factor at which a percolation channel running through the sealing surface for the first time appears. **Figure 3** visually represents how the sealing surface's contact state evolves with an increasing magnification factor. The grid on the surface is the resolution, which inversely correlates with the magnification factor: as the magnification factor increases, the resolution decreases, revealing more details of the surface topography. When the magnification continues to increase, the percolation channel also expands. The primary focus of this study is to calculate the leakage rate through the percolation channel, mainly at the critical magnification factor ζ_c. Under the differential pressure effect, the fluid flows through the channels from the high-pressure to the low-pressure side.

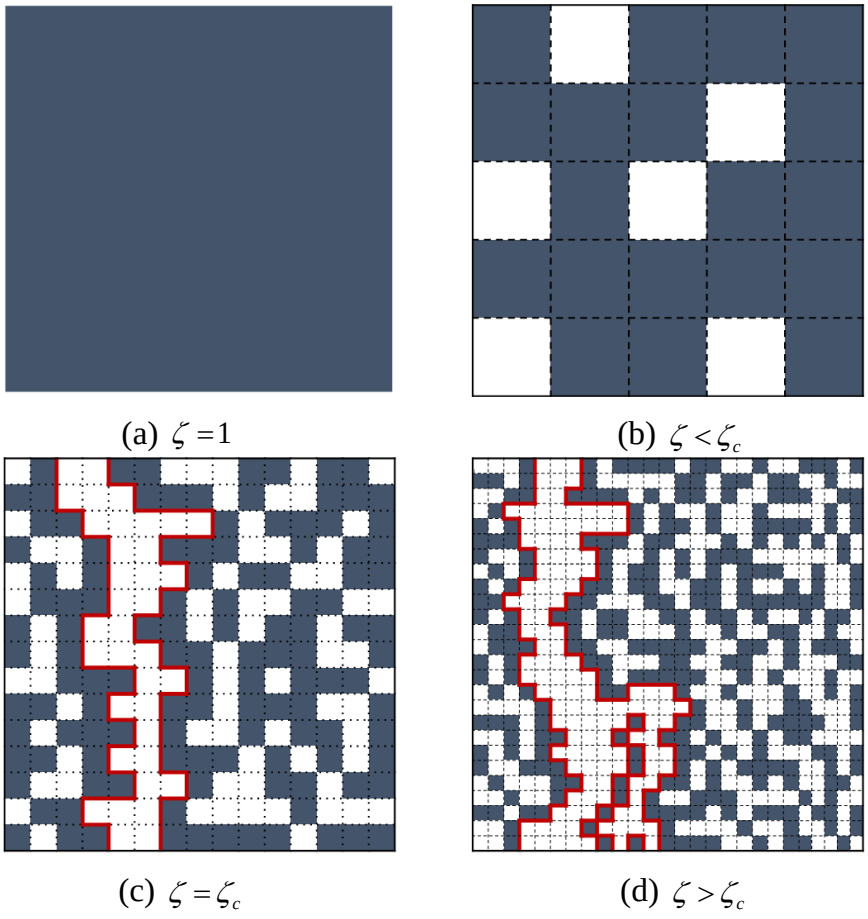

Figure 3: Relationship between separation at sealing surface and magnification factor

In this paper, to reduce the computational load of the model, the effect of differential pressure flow,

which is the leading cause of leakage in reciprocating seals, is mainly considered. The effect of shear flow is much smaller, so it is ignored. The volume flow rate of the leaking oil through the critical constriction of the penetration channel is

$$\dot{Q} = \alpha \frac{u_1^3(\zeta_c)}{12\eta} \Delta p \tag{9}$$

where α is the correction factor for the shape of the critical constriction, u_1 is the separation height at the critical constriction, ζ_c is the magnification factor at which the critical constriction occurs, η is the oil viscosity, Δp is the pressure difference between two sides of the seal. The relative contact area of a surface under a specific magnification factor is defined as the ratio of the actual contact area observed under this magnification factor to the contact area as observed under the original size, which can be expressed as

$$\frac{A(\zeta)}{A_0} = \frac{1}{\sqrt{\pi G_0}} \int_0^{p_0} d\sigma e^{-\sigma^2/(4G_0)} \tag{10}$$

where

$$G_0(\zeta) = \frac{\pi}{4} E'^2 \int_{q_0}^{\zeta q_0} dq q^3 C(q) \tag{11}$$

and the power spectral density function of the rough surface is

$$C(q) = \frac{1}{2\pi q} C^{1-d}(q) \tag{12}$$

According to [18], with the increase of the magnification factor of the rough surface, when the relative contact area decreases to 0.4, the percolation channel through the sealing surface begins to appear. Therefore, $A(\zeta)/A_0 = 0.4$ is the basis for determining the critical magnification ζ_c. The separation height at the critical constriction $u_1(\zeta)$ of the percolation channel is a crucial parameter in calculating the leakage rate through the percolation channel. When the magnification factor is reduced, some areas of the surface will re-contact; at this time, the average separation height of the channel decreases, and the constriction height can be expressed as

$$u_1(\zeta) = \bar{u}(\zeta) + \bar{u}'(\zeta) A(\zeta)/A'(\zeta) \tag{13}$$

where $\bar{u}(\zeta)$ is the average separation height between the sealing surfaces, $\bar{u}'(\zeta)$ and $A'(\zeta)$ are the derivatives of $\bar{u}(\zeta)$ and $A(\zeta)$ with respect to ς. The specific solving process of these parameters can be referred to [19].

3. SIMULATION RESULTS AND DISCUSSION

According to fractal theory, different fractal dimensions and scale parameters are selected to investigate the impact on the three-dimensional microscopic characterization of the sealing surface, as shown in **Figure 4** and **Figure 5**.

The fractal dimensions significantly affect the surface's form and structure, predominantly in roughness and texture. An increased number of fractal dimensions results in a more complex and rougher surface. The surface with fewer fractal dimensions tends to be smoother. The scale parameter determines the magnification of the rough surface. As this scale parameter decreases, the rough surface reveals more details. The rough surfaces generated have a direct impact on the contact state of the sealing surface. To analyze the wear state of the rough surface, $A(\zeta)/A_0 = 0.5$ is used as the

criterion to determine $D = 2.3$, $G = 10^{-7}$ at the compression rate of 15%.

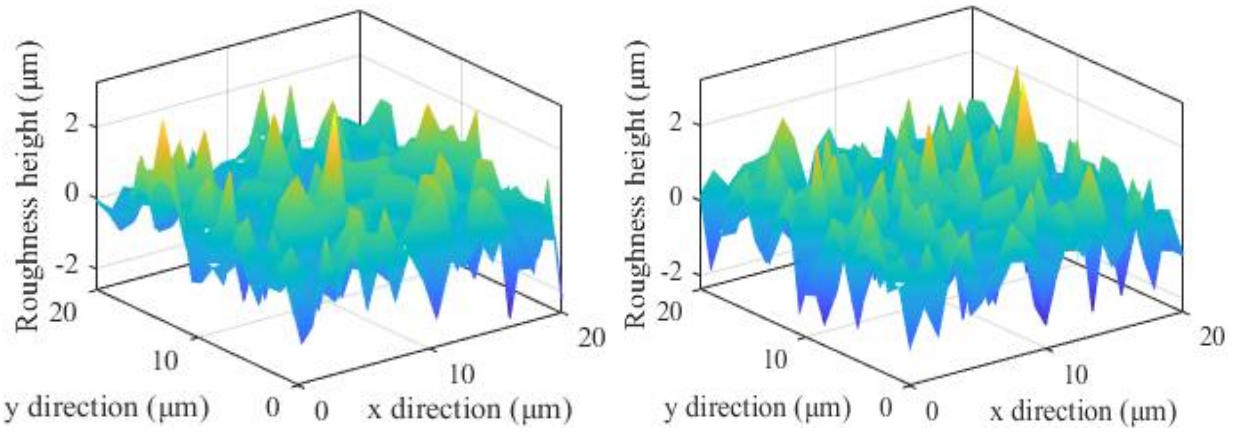

(a) $D = 2$ (b) $D = 3$

Figure 4: Rough surface topography under different fractal dimensions

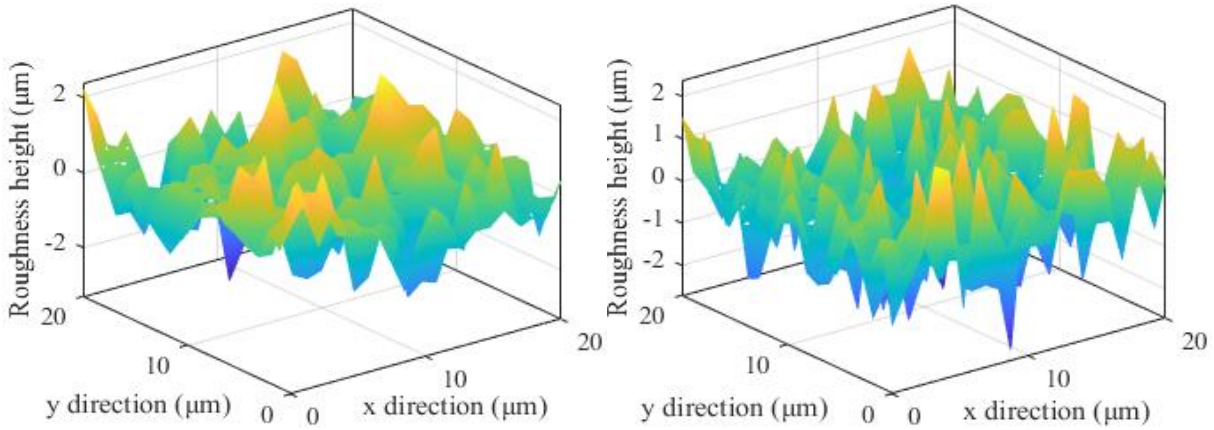

(a) $G = 10^{-6}$ (b) $G = 10^{-8}$

Figure 5: Rough surface topography under different scale parameters

The simulation parameters of the reciprocating seal in FEA are shown in **Table 1**. The piston rod and abrasive particle are made of structural steel, and the wear ring is made of PTFE. The O-ring is made of nitrile butadiene rubber (NBR), and the Mooney-Rivlin model describes its hyperelasticity.

Table 1: Simulation parameters of the reciprocating seal

Simulation parameter	Value	Simulation parameter	Value
Fluid viscosity	$0.0386 Pa \cdot s$	Sealed pressure	$15 MPa$
RMS roughness	$1 \mu m$	Elastic modulus	$550 MPa$
Rod speed	$0.05 m/s$	Stroke length	$200 mm$
Rod diameter	$18 mm$	Wear coefficient	$7.2 \times 10^{-6}\ mm^3/Nm$
Number of strokes	0,75,150,225,300	C_{10}, C_{01} of the O-ring	$0.2 Mpa$, $6.3 Mpa$
Fractal dimension	2.3	Scale parameter	10^{-7}

The rough surfaces generated in MATLAB are imported into ANSYS Workbench. We simulated the compression state of the seal by extruding the hyperelasticity rough surface with a rigid, smooth surface. **Figure 6** presents the FEA model of the created rough topography and the consequent contact state of the compressed rough surface. The axial deformation of the asperities results in most of the surface area being in a sliding state, denoted by the orange colour. The yellow regions indicate the separation between the rough and rigid surfaces, where no physical contact occurs. Most regions are

in contact at this stage, and the percolation channel has not yet formed. The sealing components within the area exhibit a robust resistance to oil leakage.

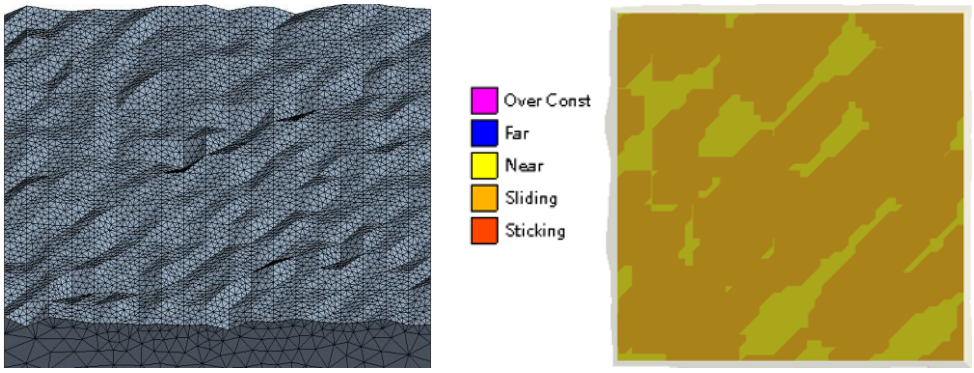

(a) FEA model (b) Contact state

Figure 6: FEA model and contact state of rough surface

The abrasive particles are incorporated into the system based on the direct compression of the rough and rigid surfaces. In hydraulic actuator systems, the size of the impurities mixed into the oil is usually 6-20 μm. This paper selects circular particles with a diameter of 6 μm and equilateral triangular particles with a side length of 10 μm. The particles are placed at the centre of a rough surface with a size of 20μm*20μm to examine the resulting Von Mises stresses following compression, as illustrated in **Figure 7**. Abrasive wear occurs in each local area of the entire sealing surface, and it can be considered that if the percolation channel is formed in the maximum contact pressure area, the channel in other areas has already been formed. Therefore, the selected local area has the highest contact pressure in the sealing length, and there is only one abrasive particle in this area. The total leakage rate can be determined by adding the leakage rate of all local areas within the circumference length of the seal.

After the wear ring is compressed by applying a load on the piston rod, the piston rod begins to move horizontally to the left. The 3D model primarily simulates the state of compression of the rough surface under compression by abrasive particles. Owing to the 3D topography revealing more detailed asperities compared to the 2D topography, the average Von Mises stress of the compressed 3D model is more significant than that of the 2D model.

In the initial compression stages, circular particles primarily interact with the wear ring through rolling contact. As the compression rate increases, the blocking effect of the asperities on the particles is enhanced, which causes the circular wear particles to transition from rolling to sliding relative to the wear ring, eventually becoming embedded in the wear ring surface and generating stress on the sealing surface. Throughout this process, the circular wear particle moves from the rough peak to the valley until the frictional force cannot overcome the asperity resistance to the wear particle, achieving stability. Under the reciprocating motion of the piston rod, the circular particle wears down the asperity on both sides until the roughness height decreases and the wear particle resumes movement following a reduction in contact stress.

The triangular wear particle is mainly sliding contact in the compression process. The upper surface of the wear particle experiences sliding friction, which embeds the corner of the triangular wear particle into the wear ring surface during the movement of the piston rod. After that, the triangular particle remains relatively static with the base surface in the subsequent friction. Given the minimal friction between the wear particle and the piston rod, the triangular wear particle does not roll with the relative movement of the two contact surfaces. Hence, abrasive particles tend to produce scratches on the wear ring surface, characterizing a pattern of cutting wear.

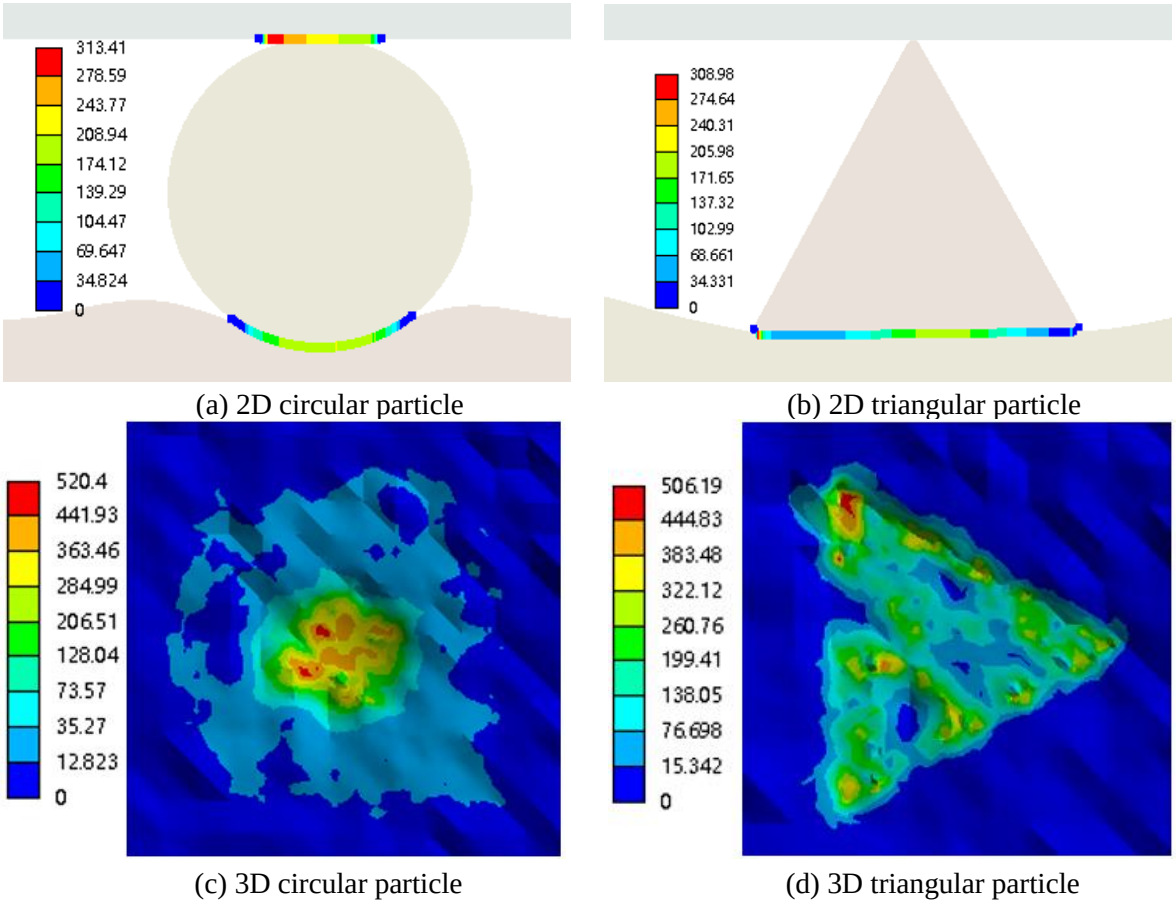

(a) 2D circular particle (b) 2D triangular particle

(c) 3D circular particle (d) 3D triangular particle

Figure 7: 2D and 3D Von Mises stress under different abrasive particles

Through the asperity pressure on the sealing surface and the Archard wear model, we can calculate the wear amount of each asperity to update the rough surface topography. The pressure distribution of the worn surface can be obtained using the worn topography for compression simulation. **Figure 8** shows that the original contact area has been worn to generate a blue percolation channel, the narrowest part of which is the critical constriction. By extracting the leakage channel and conducting a Computational Fluid Dynamics (CFD) simulation analysis of differential pressure flow, the flow rate at the critical constriction can be determined, which is very important for calculating the leakage rate of the sealing surface.

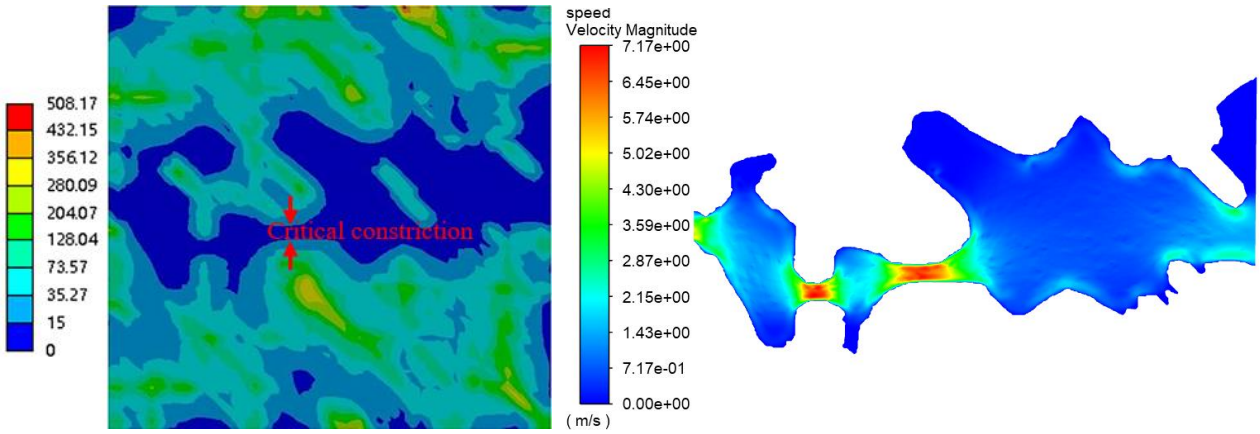

(a) Von Mises stress on sealing surface (b) CFD analysis of percolation channel

Figure 8: Numerical analysis of sealing surface and percolation channel

Operating time and fractal dimensions are two crucial parameters for surface wear. The former reflects the working conditions, and the latter reflects the surface topography characteristics. **Figure**

9 shows the average wear depth of the asperity on the rough surface of the wear ring with the operating time $T = 300s$ (corresponding to 75 strokes) and the variation of fractal dimensions under two wear particle conditions. Due to the cutting effect of triangular particles, the wear rate in the total running time is more significant than that of circle particles. With the increase of the fractal dimensions, the surface becomes progressively rougher. However, the impact on the wear induced by triangular particles remains immaterial under larger degrees of roughness. For circular wear particles, the increase in roughness height will significantly increase the hindering effect on particle movement, so the wear rate of circular particles significantly increases under large fractal dimensions.

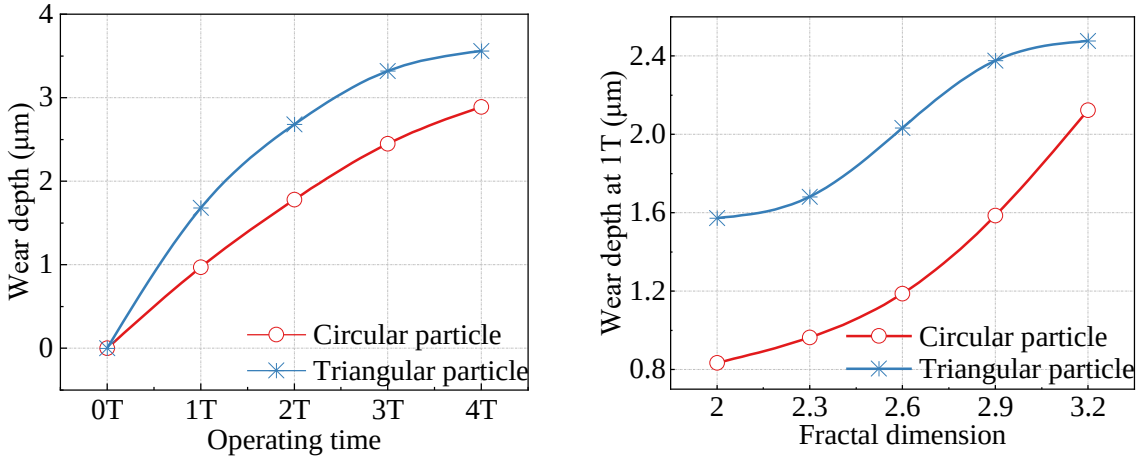

(a) Time (b) Fractal feature

Figure 9: Reciprocating seal wear depth at different serve times and fractal feature

The flow rate at the critical constriction of the percolation channel can be obtained by the wear amount and the topography evolution law, and the oil film thickness can be obtained by the numerical calculation method. **Figure 10** reflects the mapping relationship of leakage rate with operating time and fractal characteristics. Due to the large wear amount of triangular particles, the leakage rate is also more significant. It is worth noting that in the leakage rate change curve under varying operating times, the leakage rate exhibits minimal alterations at the initial stages of wear because the asperity can still undergo axial deformation under normal load at a certain height, and it is connected with other adjacent asperities to form continuous contact clusters to prevent oil leakage. As the wear process occurs, the asperity height decreases continuously, resulting in the separation in the contact area; the leakage increases rapidly in the late wear period. The influence trend of fractal dimensions on the leakage rate is consistent with the wear depth. Increasing the surface roughness harms the sealing performance, and the leakage rate increases significantly.

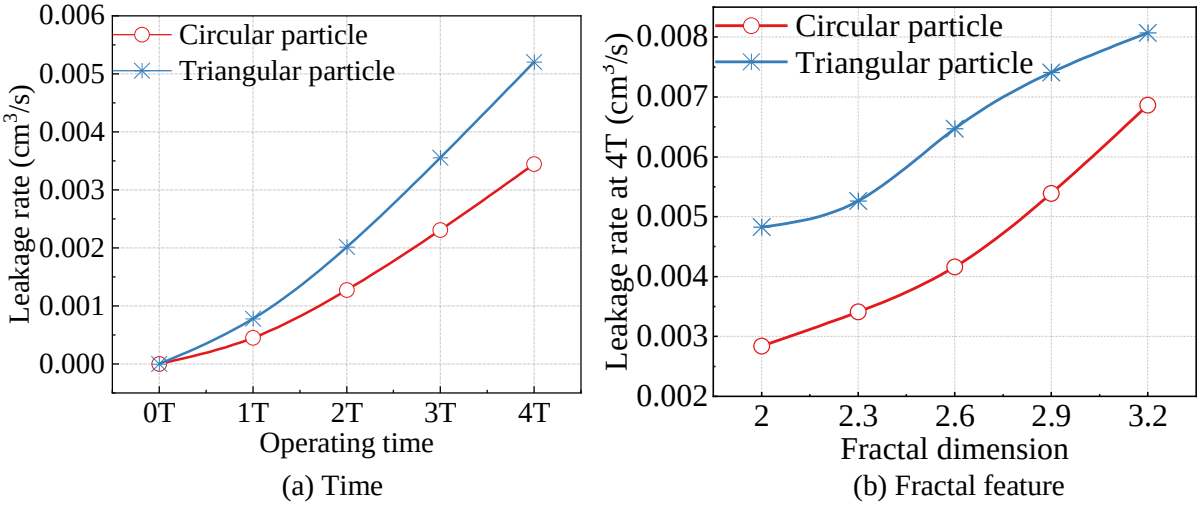

(a) Time (b) Fractal feature

Figure 10: Reciprocating seal leakage rate at different serve time and fractal feature

4. CONCLUSION AND FUTURE WORK

This study introduces a numerical approach to estimating the leakage rate of reciprocating seals experiencing abrasive wear under mixed lubrication. The circular and triangular particles are selected as research objects to obtain the Von Mises stress of the sealing surface under normal compression and with the presence of wear particles. The Archard wear model calculates the wear amount of each asperity in the abrasive wear state, and the surface topography is updated until the percolation channel through the sealing surface appears. By integrating percolation theory with CFD analysis, the flow rate and oil film thickness at the critical constriction under the influence of differential pressure flow can be obtained to calculate the leakage rate under various wear conditions.

The simulation results reveal that the triangular particle mainly plays a cutting effect, resulting in a larger wear volume than the circular particle. Moreover, the wear rate of circular wear particles increases significantly with greater surface roughness. The evolution of the leakage rate aligns with the changes in wear volume, and a running-in stage appears in the early operational phase when the difference in leakage volume is relatively indiscernible. As the wear depth intensifies, the leakage rate experiences a substantial increase.

In future work, we aim to conduct wear tests on PTFE specimens using abrasive particles of different shapes in a wide temperature range to explore the microscopic wear mechanism of the sealing surface. The topography evolution of the seal after wear can be verified by comparing the test and simulation results. The percolation theory can be adopted to establish the mapping relationship between the seal's performance degradation and topography evolution. In addition, we are currently developing an adjustable end-seal test bench, which will enable us to conduct percolation tests on worn specimen surfaces at lower sealed pressures. We expect this method to enable us to understand the leakage mechanism, predict faults, and propose optimal design schemes for sealing surfaces.

ACKNOWLEDGEMENTS

This research was supported by the China Scholarship Council (CSC) [Grant No. 202306260259].

NOMENCLATURE

A_0	Nominal contact area	n	Frequency base number
$A(\zeta)$	Contact area at magnification ζ	p_c	Asperity pressure
$C(q)$	Power spectral density function	q	Wavevector
D	Fractal dimension	$\dot{Q}$	Leakage rate
E	Elastic modulus	R	Curvature radius
F_N	Nominal load	s	Sliding distance
G	Scale parameter	u_1	Separation height at the critical constriction
h	Separation height	W_a	Wear volume
H_m	Material hardness	Δp	Pressure difference
k_a	Non-dimensional wear coefficient	σ_a	Asperity height
K_a	Wear coefficient	γ^n	Spatial frequency
K_h	Hardness coefficient	ω	Elastic deformation of an asperity
l	Asperity wavelength	ζ	Magnification factor
L	Sample length	ν	Poisson ratio
M	Number of superimposed wave layers	η	Oil viscosity

REFERENCES

[1] Nikas, G. K. (2010). Eighty years of research on hydraulic reciprocating seals: review of tribological studies and related topics since the 1930s. Proceedings of the Institution of Mechanical Engineers, Part J: Journal of Engineering Tribology, 224(1), 1-23.

[2] Salant, R. F., Maser, N., & Yang, B. (2007). Numerical model of a reciprocating hydraulic rod seal.

[3] Lorenz, B. (2012). Contact mechanics and friction of elastic solids on hard and rough substrates (Vol. 37). Forschungszentrum Jülich.

[4] Khruschov, M. M. (1974). Principles of abrasive wear. Wear, 28(1), 69-88.

[5] Wang, J., Li, J., & Ma, C. (2023). A performance degradation analysis method for a reciprocating rod seal in the wear process under mixed lubrication conditions. Proceedings of the Institution of Mechanical Engineers, Part J: Journal of Engineering Tribology, 237(3), 681-697.

[6] Peng, C., Fischer, F. J., Schmitz, K., & Murrenhoff, H. (2021). Comparative analysis of leakage calculations for metallic seals of ball-seat valves using the multi-asperity model and the magnification-based model. Tribology International, 163, 107130.

[7] Zheng, W., Sun, J., Ma, C., & Yu, Q. (2022). Percolation interpretation of film pressure forming mechanism of mechanical seal and calculation method of film pressure coefficient. Tribology International, 173, 107664.

[8] Majumdar, A., & Bhushan, B. (1991). Fractal model of elastic-plastic contact between rough surfaces.

[9] Rabinowicz, E. D. L. R. P., Dunn, L. A., & Russell, P. G. (1961). A study of abrasive wear under three-body conditions. wear, 4(5), 345-355.

[10] Koottathape, N., Takahashi, H., Iwasaki, N., Kanehira, M., & Finger, W. J. (2012). Two-and three-body wear of composite resins. Dental Materials, 28(12), 1261-1270.

[11] Liu, D., Wang, S., & Zhang, C. (2018). A multiscale wear simulation method for rotary lip seal under mixed lubricating conditions. Tribology International, 121, 190-203.

[12] Yan, W., & Komvopoulos, K. (1998). Contact analysis of elastic-plastic fractal surfaces. Journal of applied physics, 84(7), 3617-3624.

[13] Li, J. S., Tang, Y., Li, Z. T., Ding, X. R., & Li, Z. (2017). Study on the optical performance of thin-film light-emitting diodes using fractal micro-roughness surface model. Applied Surface Science, 410, 60-69.

[14] Fischer-Cripps, A. C. (1999). The Hertzian contact surface. Journal of materials science, 34(1), 129-137.

[15] Liu, Y., Liskiewicz, T. W., & Beake, B. D. (2019). Dynamic changes of mechanical properties induced by friction in the Archard wear model. Wear, 428, 366-375.

[16] Yuan, Y., Gan, L., Liu, K., & Yang, X. (2017). Elastoplastic contact mechanics model of rough surface based on fractal theory. Chinese Journal of Mechanical Engineering, 30(1), 207-215.

[17] Persson, B. N. J. (2007). Relation between interfacial separation and load: a general theory of contact mechanics. Physical review letters, 99(12), 125502.

[18] Yang, C., & Persson, B. N. J. (2008). Contact mechanics: contact area and interfacial separation from small contact to full contact. Journal of Physics: Condensed Matter, 20(21), 215214.

[19] Persson, B. N. J., & Yang, C. (2008). Theory of the leak-rate of seals. Journal of Physics: Condensed Matter, 20(31), 315011.